AWARD NUMBER: BC151687

TITLE: **The role of extracellular vesicles in metastasis**

PRINCIPAL INVESTIGATOR: Gabriela G. Loots

CONTRACTING ORGANIZATION: Lawrence Livermore National Laboratory
7000 East Avenue
Livermore, CA 94550-9698

REPORT DATE: Jan 2020

TYPE OF REPORT: Final Report

PREPARED FOR: U.S. Army Medical Research and Development Command
Fort Detrick, Maryland 21702-5012

This work was performed under the auspices of the U.S. Department of Energy by Lawrence Livermore National Laboratory under Contract DE-AC52-07NA27344.

REPORT DOCUMENTATION PAGE

Form Approved
OMB No. 0704-0188

1. REPORT DATE	**2. REPORT TYPE**	**3. DATES COVERED**
Jan 2020	Final Report	10/1/2016-9/30/2019

4. TITLE AND SUBTITLE
The role of extracellular vesicles in metastasis

5a. CONTRACT NUMBER
10922451

5b. GRANT NUMBER
BC151687

5c. PROGRAM ELEMENT NUMBER

6. AUTHOR(S)

Gabriela G. Loots

E-Mail: loots1@llnl.gov

5d. PROJECT NUMBER

5e. TASK NUMBER

5f. WORK UNIT NUMBER

7. PERFORMING ORGANIZATION NAME(S) AND ADDRESS(ES)

United States Department of
Energy Livermore Office
7000 East Avenue
Livermore, CA 94550-9698

8. PERFORMING ORGANIZATION REPORT NUMBER

9. SPONSORING / MONITORING AGENCY NAME(S) AND ADDRESS(ES)

U.S. Army Medical Research and Materiel Command
Fort Detrick, Maryland 21702-5012

10. SPONSOR/MONITOR'S ACRONYM(S)

11. SPONSOR/MONITOR'S REPORT NUMBER(S)

12. DISTRIBUTION / AVAILABILITY STATEMENT

Approved for Public Release; Distribution Unlimited

13. SUPPLEMENTARY NOTES

14. ABSTRACT

The proposed work addresses the dire need for new platforms for ESV isolation and precise, quantitative characterization of each cancerous ESV subpopulation's role in cargo transfer. Specifically, we aim to (1) optimize an existing microfluidic separation platform to efficiently isolate ESV subpopulations (from the cells and from each other) originating from breast cancer cell lines with a range of metastatic character, (2) engineer breast cancer cell lines with fluorescent and radiolabeled ESV sub-populations for individual tracking, and (3) use accelerator mass spectrometry (AMS), which allows extremely sensitive rare-molecule detection, to quantify low levels of tumor-derived RNA transferred via ESVs to osteoblasts. These bone cells represent the most common tissue target for breast cancer metastasis, and we will mimic ESV-mediated cancer invasion and metastasis by growing the cancerous and bone cells together in a trans-well cell co-culture system. The use of these molecular and physical tools in combination specifically to address cancer invasiveness and mechanisms of metastasis is unprecedented. This study will yield the first quantitative data on which ESV subpopulations (exosomes, MVs, or oncosomes) manipulate the tumor microenvironment, the ESV cargo transferred, and how this differs across the range of cell metastatic potential.

15. SUBJECT TERMS

16. SECURITY CLASSIFICATION OF: U			**17. LIMITATION OF ABSTRACT**	**18. NUMBER OF PAGES**	**19a. NAME OF RESPONSIBLE PERSON** USAMRMC
a. REPORT	**b. ABSTRACT**	**c. THIS PAGE**	UU		**19b. TELEPHONE NUMBER** *(include area code)*
U	U	U			

Standard Form 298 (Rev. 8-98)
Prescribed by ANSI Std. Z39.18

Table of Contents

Page

- **INTRODUCTION:** *Narrative that briefly (one paragraph) describes the subject, purpose and scope of the research.*

The release of extracellular vesicles (ESVs) from high grade, aggressive forms of human cancer cells into their surroundings has become increasingly recognized as a feature of tumor biology, but what promotes ESV release, what cargo different ESV subpopulations carry, and what roles ESV contents have in tumor progression remains largely unknown. One hindrance to the lack of progress has been the scarcity of methods available to purify large quantities of ESV subpopulations intact, without cellular contaminants or without damaging the cargo. A second hindrance has been the lack of quantitative methods for measuring very small amounts of DNA and RNA transferred from tumor cells to the surrounding cells. As cancer progresses, the surrounding microenvironment co-evolves with the tumor through continuous paracrine cross-communication, thus creating a dynamic signaling circuitry that promotes cancer initiation, growth, drug resistance, metastasis and ultimately organ failure and death. The stromal components that include endothelial cells, pericytes, fibroblasts, various classes of leukocytes, and extracellular matrix are likely to receive 'executive signals' from the tumor in the form of proteins, mRNAs, ncRNAs, miRNAs and DNA to promote phenotyping changes in the stromal components that benefit the tumor. If we can detect the signals propagated from the tumor cells to the stroma, we can begin to formulate new testable hypotheses on how cancer cells manipulate their microenvironment to develop an aggressive phenotype. To address these shortcomings, the project has three specific aims:

Aim 1. Optimize an existing microfluidic platform developed at LLNL to efficiently separate different ESV subpopulations from different breast cancer cell lines with varying metastatic character [MDA-MB-231 (highly invasive); MCF7 (moderately invasive); MCF10A (non-tumorigenic)].
Aim 2. Engineer breast cancer cell lines with fluorescent and radiolabeled ESV subpopulations.
Aim 3. Use accelerator mass spectrometry (AMS) technologies to quantify low levels of tumor-derived RNA transferred via ESVs to osteoblasts and characterize their functions in promoting invasion.

- **KEYWORDS:**

Breast cancer, extracellular vesicles, exosome, MDNA-MB-231, MCF7, MCF10A, 4T1, metastasis

- **ACCOMPLISHMENTS:**
  - **What were the major goals of the project?**

	Year 1	Year 2	Year 3
Specific Aim 1. Optimize an existing microfluidic platform developed at LLNL to efficiently separate different ESV subpopulations from different breast cancer cell lines with varying metastatic character [MDA-MB-231 (highly invasive); MCF7 (moderately invasive); MCF10A (non-tumorigenic)].			
Task 1A: Verify microfluidic separation performance of ESVs from host cells and debris using existing acousto-fluidic devices with each of the 3 breast cancer cell lines			
	1a: Generate mixed cell-vesicle samples by growing cells in serum-starved media; process samples through separation device at a range of flow and pressure-field parameters and assess separation efficiency and purity by cell counting, SEM and fluorescence		

	microscopy and qPCR.		
Task 1B: Determine optimal separation strategy for oncosome population in each of the 3 breast cancer cell lines; verify bead-complexed separation of populations			
	1b: In tandem with Task 1a, for each cell line, determine whether oncosomes are best grouped with "large" (cells) or "small" group (microvesicles and exosomes), i.e. conditions at which largest fraction of oncosomes are recovered.	Label subpopulation-specific ESV surface markers (e.g. CD63) with antibody-derivatized polystyrene micro-spheres and verify purity and separation efficiency of resulting subpopulation separation by qPCR and SEM.	
Milestone #1: Tabulate separation parameters (flow rate, actuation voltage and frequency) for purifying ESVs vs. host cells/debris for each of 3 cell lines; publication on acoustic device performance			
Task 1C: Design and fabricate acoustic separator chips specifically optimized for isolation of ESV subpopulations			
		1c: From results of Tasks 1a and 1b, generate new photo-masks, and fabricate new microfluidic devices, optimally configured to isolate ESV subpopulations, ideally in a single pass through the device.	
Milestone #2: Fabricate 30-50 new microfluidic devices based on optimized design parameters.			
Task 1D: Verify isolation and purification of multiple ESV subpopulations by optimized acoustofluidic device			
		1d: Using mixed cell-vesicle samples grown from serum-starved media, pass samples through optimized devices and assess separation efficiency, purity and recovery.	Continue using acoustic devices to generate pure ESV samples for supporting the efforts in Tasks 2 and 3.
Milestone #3: A functional automated separation platform capable of rapid recovery of individual ESV subpopulations from bulk cell culture samples.			
Milestone #4: Publication reporting results of platform development and novel findings on ESV shedding rates and quantities in breast cancer cell lines of different metastatic character.			
<u>Specific Aim 2:</u> ***Engineer breast cancer cell lines with fluorescent and radiolabeled ESV subpopulations.***			
Task 2A: Engineer [MDA-MB-231 (highly invasive); MCF7 (moderately invasive); MCF10A (non-tumorigenic)] cell lines to express fluorescent markers that discriminate exosomes from			

microvesicles.			
2a: Create DNA constructs that express CD63 or CD9 [exosome markers] fusion proteins with mKate, a far red fluorescent protein and CD40 or CD63 [microvesicle marker] fusion proteins with eGFP, an enhanced green fluorescent protein	Where available fusion protein clones will be purchased, transfected into MDA-MB-231; MCF7; MCF10A cells and selected for stable transfected cell lines. If not available for purchase, the full length cDNA clones will be obtained from IMAGE and subcloned to insert mKate or eGFP in frame to create fusion constructs	Stable transfected cell lines with one exosome and one microvesicle specific markers will be characterized using imaging, western blots, and immunoprecipitation to confirm the location of the fluorescent protein.	
Milestone #5: Create new MDA-MB-231, MCF7, MCF10A subclonal cell lines that express fluorescent markers that allow us to discriminate between exosomes (red) and microvesicles (green). Each breast cancer cell line will be positive for 2 transgenes [mKate+; eGFP+]			
Task 2B: Engineer [MDA-MB-231 (highly invasive); MCF7 (moderately invasive); MCF10A (non-tumorigenic)] cell lines to express a transgene for uracil phosphoribosyltransferase [UPRT].			
2b: Transfect DNA construct that expresses UPRT into MDA-MB-231; MCF7; MCF10A cells and select for stable cell lines.		MDA-MB-231; MCF7; MCF10A cells lines expressing mKate or eGFP fusion proteins will be transfected with UPRT vectors, and select for triple transgenic lines [mKate+; eGFP+; UPRT+]	
Milestone #6: Create new MDA-MB-231, MCF7, MCF10A subclonal cell lines that express fluorescent markers that allow us to discriminate between exosomes (red) and microvesicles (green) and also express UPRT. Each breast cancer cell line will be positive for 3 transgenes [mKate+; eGFP+; UPRT+]			
<u>Specific Aim 3:</u> ***Use Accelerator Mass Spectrometry (AMS) technologies to quantify low levels of tumor derived RNA transferred via ESVs to osteoblasts, and characterize their functions in promoting invasion***			
Task 3A: Determine if cancer cells derived microvesicles or exosomes carry RNA			
		3a. Different ESV subpopulations derived from triple transgenic cancer cell lines and cultured with ^{14}C-thiouracil will be isolated using microfluidic device and the ^{14}C-level will be quantified using AMS. Since only RNA will be labeled with ^{14}C, only	Quantify the amount of RNA packaged in ESV in the 3 triple transgenic cancer cell lines cultured with ^{14}C-thiouracil. Optimize culture conditions to enrich for ESV populations that carry RNA, to obtain sufficient RNA for

		ESV populations positive for ^{14}C will be used to isolate RNA and sequence the RNA	sequencing
Milestone #7: Determine which ESV subpopulation has mRNA cargo			
Task 3B: Determine if cancer cells derived microvesicles or exosomes are taken up by osteoblasts			
3b:			3b: Triple transgenic lines created in 2b will be co-cultured with osteoblasts, at different time points [6 hours, 24 hours, 48 hours, 96 hours] the RNA will be isolated from osteoblasts and ^{14}C will be quantified to determine if RNA was transferred from cancer cells to the bone cells. RNA will be further isolated and sequenced
Milestone #8: Identify whether tumor cells package mRNA randomly into ESVs, or whether there is a rationale and metastatic tumors package 'unique' mRNA species that are more likely to influence their environment			
Milestone #9: Publication reporting results of ESV differences in transferring RNA to osteoblasts, among breast cancer cell lines with different metastatic character.			

- **What was accomplished under these goals?**

Specific Aim 1*. Optimize an existing microfluidic platform developed at LLNL to efficiently separate different ESV subpopulations from different breast cancer cell lines with varying metastatic character [MDA-MB-231 (highly invasive); MCF7 (moderately invasive); MCF10A (non-tumorigenic)].*

In task 1a we aimed to verify microfluidic separation performance of ESVs from host cells and debris using existing acousto-fluidic devices with each of the 3 breast cancer cell lines. Towards our goal of developing microfluidic methods of ESV we (1) characterized the separation efficiency of three different cell types. (2) assessed different methods for exosome and micro vesicle quantification and (3) demonstrated moderate separation using surrogate particles to determine feasibility of separation exosomes bound to immunocapture beads and microvesicles.

First, we designed and manufactured a new batch of microfluidic acoustophoretic separators. This design iteration tested several strategies to maximize particle residence time within the chip for improving separation while maintaining high volumetric flow. Next, we fully characterized these devices by determining the resonant frequency, and flow focusing characteristics with 7 µm polystyrene beads. This maintenance and development was essential to ensure we had an adequate stock of well calibrated devices for biological tests.

We further quantified the separation of three different cell types into cell outlet to determine the optimal conditions to remove cells and cell debris from vesicle samples. Overall, we found slight differences in the different cell types, with MCF7As requiring the highest voltage to achieve separation (**Figure 1**).

To evaluate the performance of our acoustic separation on extracellular vesicles we first needed to develop methods to measure different populations of vesicles. Therefore, a significant effort was invested in identifying ways to quantify and measure vesicles.

Figure 1. Separation efficiency of cells and cell debris from smaller constituents (extracellular vesicles). Separation efficiency is defined as the number of cells exiting from the Large Particle Outlet (LPO) scaled by the total number of cells recovered after separation. The experimental data is fit to a sigmoid curve. Depending on the cell type different voltages are required to remove cells and cell debris. Samples are run at 100 µl/minute.

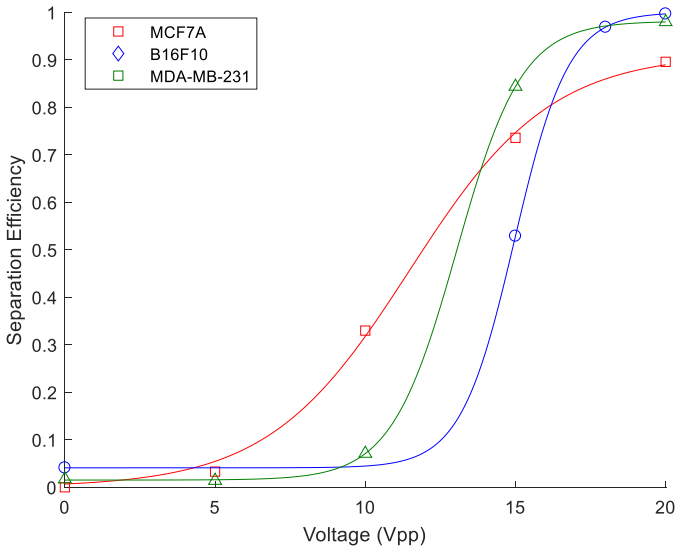

To identify exosomes we first concentrated exosomes using standard techniques of 0.2 µm filtration and ultracentrifugation. Then, we used a lipophilic dye to fluorescently label all vesicles. Next, immunological CD9 and CD63 beads were incubated with the exosomes, and samples were quantified by FACS (**Figure 2**).

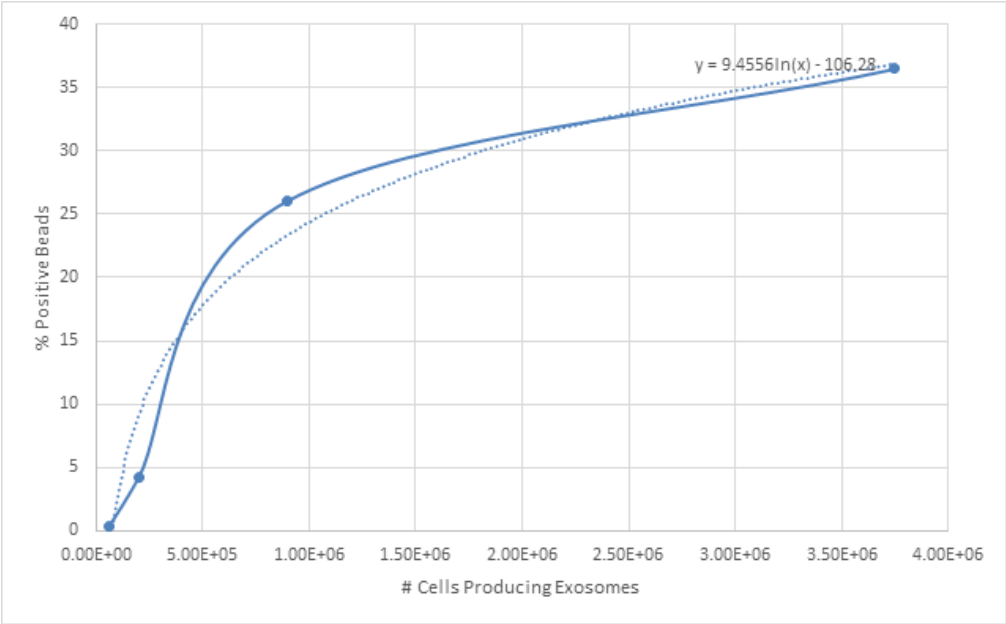

Figure 2: Calibration curve of positive signal versus number of cells using bead method to quantify exosomes.

Using these methods, we ran exosome samples under conditions to remove cell and cell debris (100 µL/minute flow rate, 20Vpp) and showed that exosomes exit out of the vesicle Small Particle Outlet (SPO). Results indicated that exosomes and cells can readily be separated using this technique (**Figure 3**).

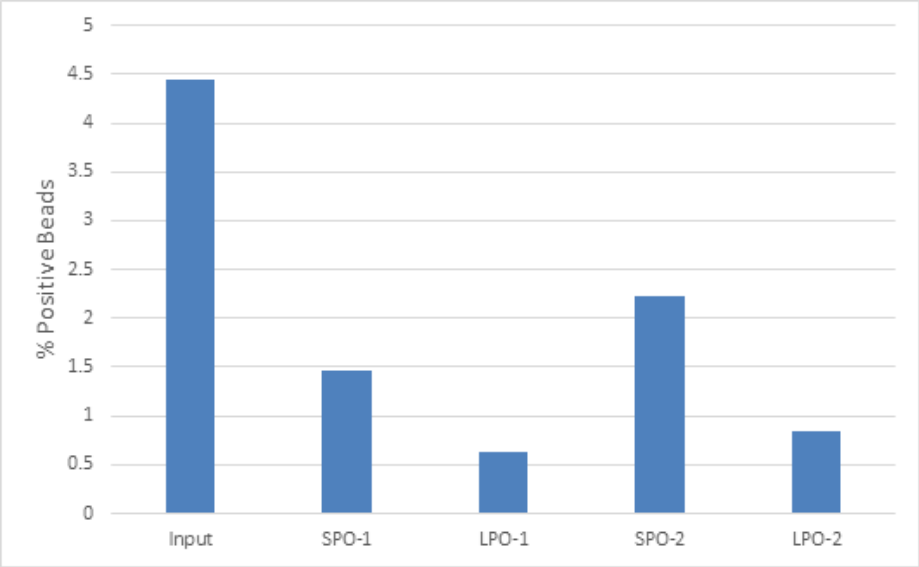

Figure 3: Relative output from two different runs through the acoustophoretic separator at conditions for cell separation. The SPO fractions have more positive beads than the LPO fraction, indicating that exosomes will exit from the SPO while cells will exit from the LPO.

In task 1b we proposed to isolate large oncosome populations (> 5 µm) from smaller microvesicle and exosome populations using immunological beads combined with acoustic separation. Defining oncosome population has been more challenging, therefore we have focused primarily on smaller microvesicle and exosome populations. Our proposed experimental plan using acoustic separation to isolate large oncosomes and immunologically labeled vesicle subsets in a single device was expected to streamline vesicle purification (Tasks 1b and 1c). Since we could not "find" oncosomes, we experimented with using acoustophoretic separation to isolate different ESV populations using immunological beads. We first demonstrated the potential to use acoustophoretic separation to separate ESVs bound to beads and free ESVs. However, we determined later that this method was not superior to existing immunological ESV purification using magnetic beads. Existing methods using functionalized magnetic beads proved to be superior in throughput as well as limiting the dilution of exosome samples. Furthermore, the dearth of isolation and purification techniques for ***functional*** exosomes become apparent to us and we saw a pressing need for methods optimized for basic science applications. Widely used exosome purification techniques using immunological markers were ill-suited for fundamental exosome research since they inherently select for specific subsets of exosomes, limiting our ability to draw general conclusions and interrogate the full spectrum of exosomes produced by various cells. Additionally, removing attached antibodies was challenging, thus we recognized that the basic research needs would benefit from label free vesicle purification for functional vesicle recovery. Furthermore, high forces generated using ultracentrifugation, the gold standard for exosome concentration, can affect exosome morphology and is expected to negatively impact exosome function [1, 2] Therefore, in FY18 we shifted our focus towards identifying label-free methods of concentrating and purifying exosomes as described below.

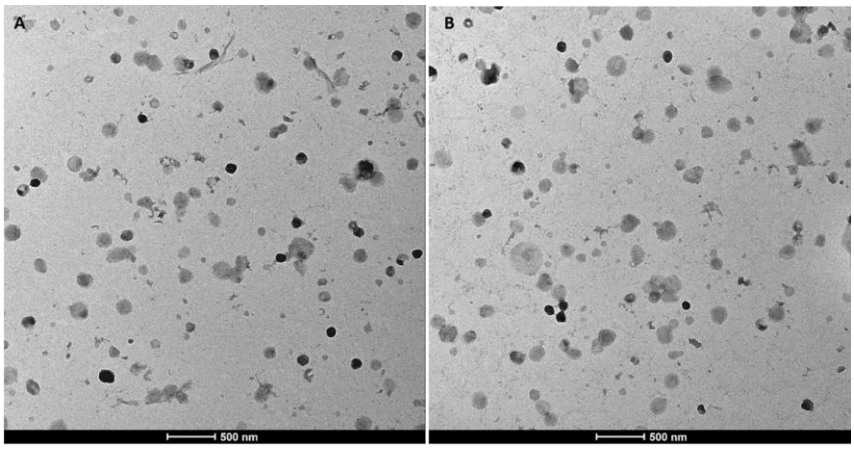

Figure 4. **TEM images of ESVs isolated using one processing step** A) concentrating pipette and B) ultracentrifugation.

We assessed different concentration and recovery methods for isolating functional exosomes. We have looked at two widely used methods of vesicle concentration and purification: Ultracentrifugation, the gold standard for exosome isolation [3], and ExoQuick, an ethylene glycol precipitation-based method. We further investigated two size-based methods which have only recently been applied to vesicle purification: (1). InnovaPrep's Concentrating Pipette: This is an emerging filtration-based technique, which isolates particles on

size selective filters and then recovers them using a high-pressure aerosol elution foam designed to gently and completely remove particles from the membrane; and (2). Concentrating and purifying exosome samples through dialysis and evaporation.

Comparison of different concentrating methods: Ultracentrifugation, Precipitation- ExoQuick, Filtration and Elution- Concentrating Pipette

To investigate different methods of label-free ESV concentration, we utilized transmission electron microscopy (TEM) analysis to assess each of these different techniques: Ultracentrifugation, Precipitation- ExoQuick, Filtration and Elution- Concentrating Pipette **(Figure 4**). Initial tests optimizing the extraction parameters using the Concentrating Pipette were performed using conditioned media from B16F10 cells, as B16F10 abundantly produce exosomes. Results measuring exosomes isolated by ultracentrifugation using dynamic light scattering showed more signal from exosomes isolated from B16F10s compared to numerous other cell lines including: MDA, E0771, PC3, or 4T1 cells. Thus, we used these exosomes for subsequent tests to optimize workflow and assay concentration techniques. Media was conditioned by serum starving cells for 24 hours (h) to induce exosome production and collected. Samples were spun on the benchtop to remove cell debris, then 0.2 um filtered, and processed via ultracentrifugation (200,000G for 2 hours), or using the concentrating pipette. To assess how multiple processing steps affected exosome isolation, additional samples were subject to two rounds of ultracentrifugation, and ultracentrifugation followed by using the concentrating pipette (**Figure 5**). After the first processing step, the concentrated exosomes were resuspended in the original volume and processed with the second processing step. All samples were eluted in 150 µL of buffer and stored at -80 C until TEM analysis. To analyze the particle size and concentration, we selected the best image for each condition and manually fit ellipsoids to vesicles (**Figure 6**).

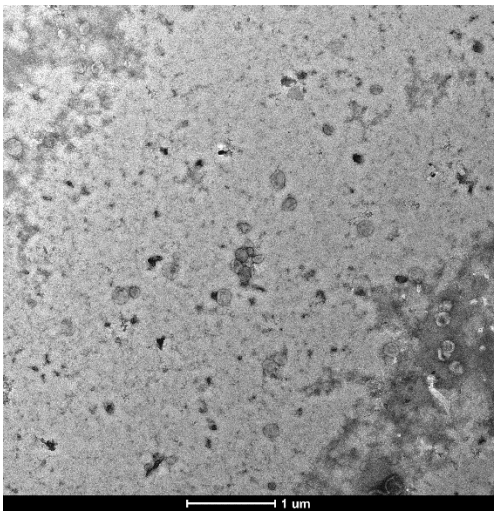

Figure 5: **TEM images of ESVs isolated with two rounds of ultracentrifugation**. No ESV were detected in samples processed by ultracentrifugation followed by the concentrating pipette.

From these results we concluded that (1) The quantity and size of vesicles was comparable between concentrating pipette and single round of ultracentrifugation and (2) Multiple processing steps (two rounds of ultracentrifugation or ultracentrifugation followed by concentrating pipette) significantly reduced the quantity and the quality of isolated vesicles. TEM images from both cases show increased debris and reduced counts of vesicles. No ESVs were identified in samples subjected to ultracentrifugation followed by the concentrating pipette, suggesting that the different vesicle populations are selected for using the different isolation techniques and processing with both techniques resulted in a loss of all ESVs.

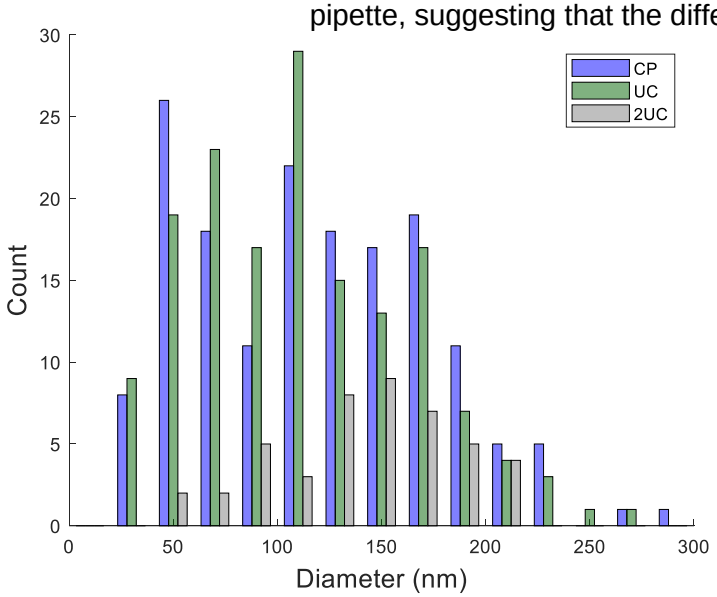

Figure 6. Sizes of ESVs collected via concentrating pipette (blue), ultracentrifugation (green) and two rounds of ultracentrifugation (gray). Note that a larger field of view was analyzed for the sample processed by two rounds of centrifugation. The number of ESVs per imaged area: concentrating pipette: 843 particles per mm^2; ultracentrifugation: 817 particles per mm^2; two rounds of ultracentrifugation: 143 particles per mm^2

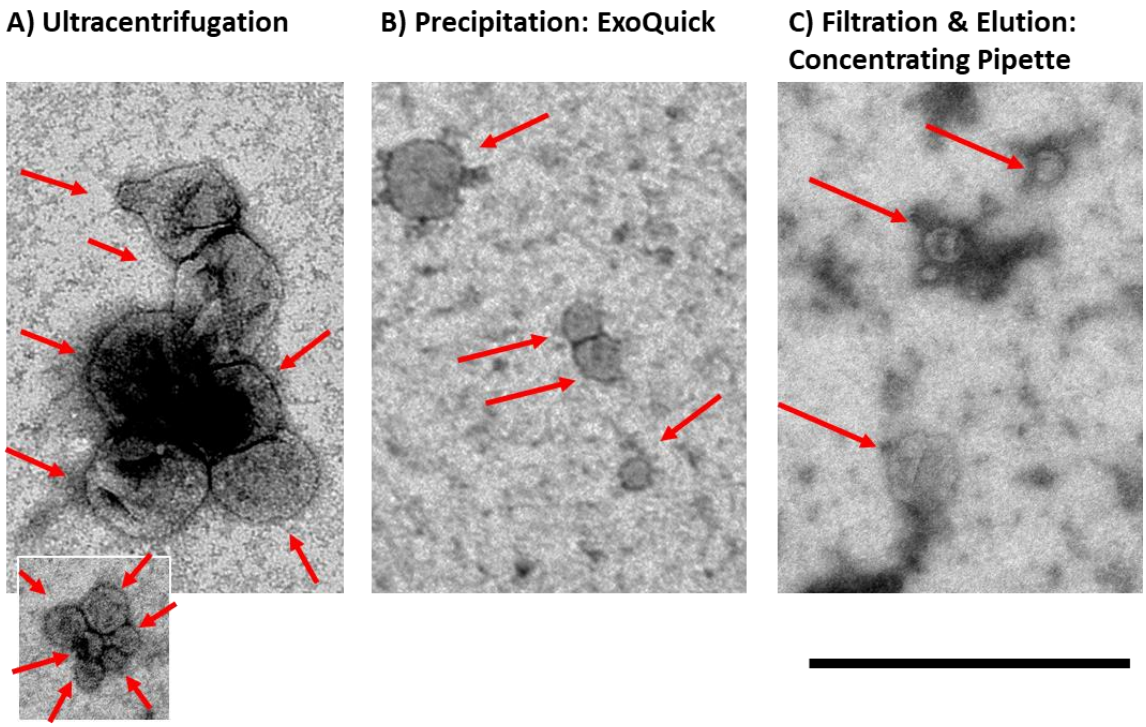

Figure 7: ESVs isolated from 4T1 breast cancer cells using different techniques. Red arrows indicate ESVs. Scale bar is 500 nm. A) Different fields of view of samples processed via ultracentrifugation showed dramatically different sized ESVs. Two different images are presented for the ultracentrifugation case to capture this.

Overall, these results suggested that the Concentrating Pipette may be an alternative method to isolate exosomes with performance comparable to ultracentrifugation. Thus, we moved forward with characterizing exosomes from breast cancer cells. We generated exosomes from 4T1 mouse breast cancer cell lines as described above. The 4T1 ESVs were isolated with more debris and at lower concentrations than those from B16F10 cells. This result was in line with our previous results indicating that B16F10s produce greater amounts of ESVs. **Figure 7** shows representative images of ESVs isolated using each technique. ESVs isolated *via* the concentrating pipette or the ExoQuick kit appeared somewhat more uniform in size than exosomes isolated using ultracentrifugation, which shows a large range of ESV sizes (**Figure 7a**). However, due to the small sample size of imaged ESVs it was not possible to quantitate size differences between the different conditions.

Development of Evaporative Concentration and Dialysis

In task 1c we proposed to fabricate acoustic separator chips for the isolation of ESV subpopulations. Given the change of direction of the project in FY18, we instead worked towards developing methods and devices for ESV concentration and purification from conditioned cell media to complement our other work described. Key features of an ideal exosome isolation method for functional exosome recovery were (1) At least 10-fold ESV concentration; (2) Process multiple milliliters of sample in a reasonable time frame (<1 day). (3) Label-free; (4) Removal of protein contaminants and (5) Less force/more gentle than ultracentrifugation.

Recently, hydrostatic filiation dialysis has been used for large volume concentration of concentrate exosomes from urine [4]. In this technique, commercial cellulose ester dialysis tubing was filled with the vesicle sample and suspended vertically in air. The hydrostatic pressure pushes the solvent and species smaller than the molecular weight cut off through the membrane while retaining larger species within the tubing. We sought to apply this technique to volumes suitable for small scale cell culture experiments to complement our other cell culture work. Mirroring their process, we experimented with using a model bead system with 200 and 1000nm fluorescent beads suspended in cell culture media to represent different vesicle populations, which could be

quantitatively measured to determine recovery and concentration. To enhance the concentration rate, we experimented with applying pressure to the sample to enhance the pressure inside and outside of the tubing. We further found that performing these experiments in air causes the cellulose membrane to dry out which affects the pore size and membrane strength. Therefore, at higher pressures, it was necessary to submerge the device in buffer. We filled 300kDa cellulose ester dialysis tubing with 8-10 ml of sample and tested different applied pressures, both submerged in buffer or in air.

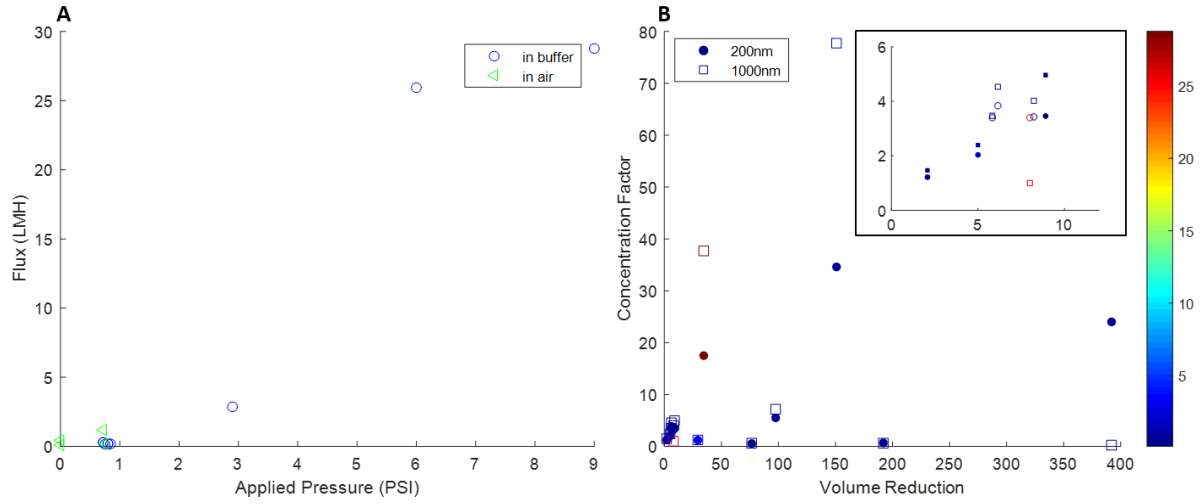

Figure 8. **Tests with enhanced hydrostatic filtration**. A) Flux through the membrane as a function of applied pressure demonstrates increased throughput at higher applied pressures. B) Concentration factor vs. Volume reduction for 200 and 1000 nm beads. Color represents flux in LMH, filled markers are performed in air, open markers are performed in buffer. Inset is enlarged plot at low volume reductions.

Samples collected in the membrane were compared to input samples by measuring fluorescence. Our initial tests demonstrated that enhanced throughput was possible by increasing the applied pressure to the sample (**Figure 8A**). These tests indicated that overall, larger particles were more efficiently retained and concentrated within the dialysis tubing as expected. At low volume reductions, we see an increase of concentration with increasing volume reduction (**Figure 8B**, inset). The concentration factor is slightly less than the volume reduction due to particle losses. We expect most loss particles are retained on the membrane rather than passing through the membrane, as no particles were detected in solution passing through the membrane, which is consistent with reported vesicle behavior using this technique [4]. At higher volume reductions results were however extremely inconsistent. While it was possible to achieve extreme concentration and volume reduction (best results: 35x concentration of 200 nm beads, 78x concentration of 1000 nm beads and 150x volume reduction), numerous experiments resulted in little to no concentration (**Figure 8B**). When the volume was dramatically reduced, particles were observed sticking to the membrane and stuck in the region where the dialysis tubing was sealed and were not recovered reliably. Our results indicated that 10x vesicle concentration was possible, however, concentrating volumes to less than 1 ml was not feasible using this technique in its current form. While this method worked well for large, dilute urine samples, to adapt it for smaller cell culture volumes we needed to increase the fluidic control and improve sample recovery.

Thus, we next developed a dialysis device with defined channels that allowed us to precisely manipulate fluid on all sides of the membrane (**Figure 9).** The design of this device draws on microfluidic platforms for ESV isolation and filtration [5, 6] designed for diagnostic applications, but sought to process larger volumes. To achieve gentle ESV isolation, we aimed to employ evaporation for concentrating [7-9], and dialysis [10] to remove contaminants and maintain favorable conditions (i.e. keeping the osmotic pressure stable and limiting the co-concentration of salts and other species). We integrated this device with various automated fluidic handling valves, pressure pumps, vacuum sources, and syringe pumps which allowed us to create well defined sample concentration and recovery procedures [11] to increase the repeatability and efficiency of ESV isolation.

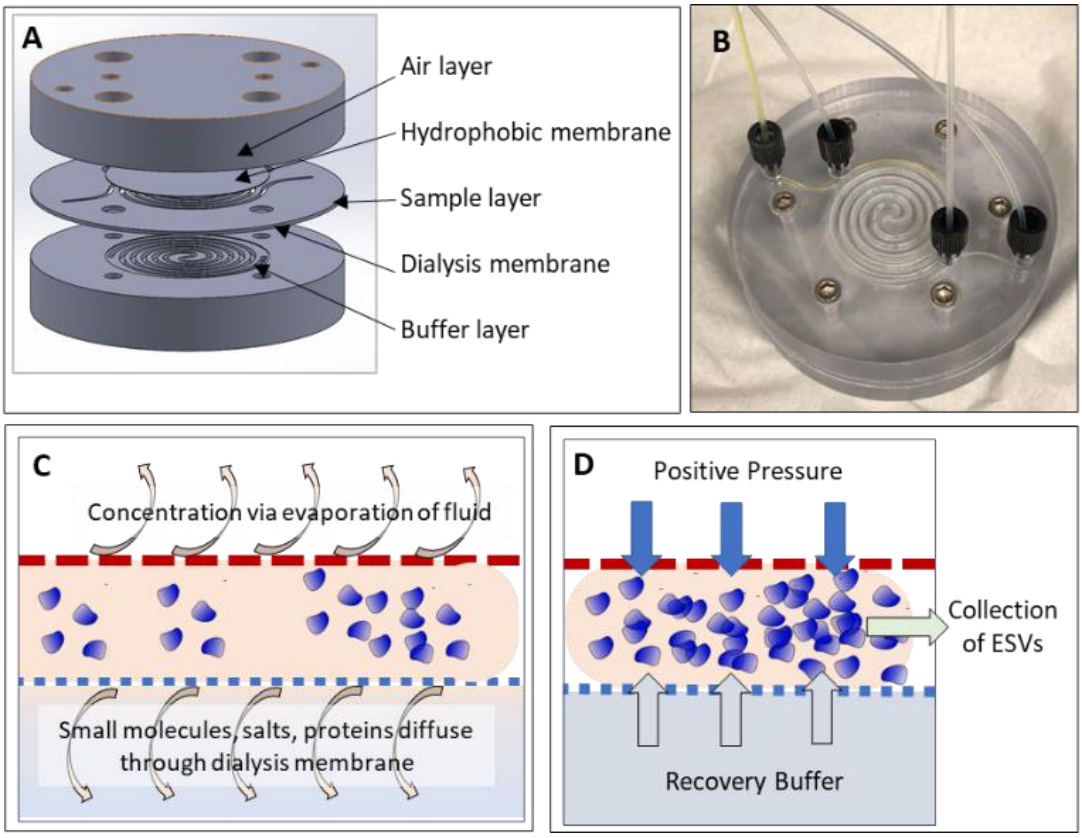

Figure 9. **Second Generation Evaporative Dialysis Device**. A) Exploded view of device stack with custom manufactured parts. B) Image of device with fluidic inputs and outputs connected for the sample and air layer (buffer layer ports are on bottom of device). C) Schematic of concentration and purification during sample processing. D) Schematic of ESV recovery.

Specific Aim 2: Engineer breast cancer cell lines with fluorescent and radiolabeled ESV subpopulations.

Towards our goal of engineering cell lines we: (1) engineered MDA-MB-231 cell line to express CD9-, CD63-, and CD81-GFP fusion proteins; (2) demonstrated that engineered cells can be sorted by FACs and (3) showed fusion protein expression by Western blot.

Upon original design of the fusion protein constructs, it was found that the inconsistent expression of specific markers on exosomes may pose future limitations to both the ability to capture and localize exosome transport. Classic exosome markers such as Tsg101, Rab-5b, and CD-63 were shown to produce variable expression depending on origin of the exosome. To circumvent this heterogeneity, we created a plasmid construct containing GFP fusion proteins for 3 common exosome tetraspanin markers (CD9, CD63, and CD81) [12] in tandem (pLLNL-exo-GFP) in order to both increase fluorescent intensity per exosome and label a more comprehensive population of exosomes (**Figure 10a**). A MDA-MB-231 cell line stably expressing pLLNL-exo-GFP was first created and validated for GFP expression *via* flow cytometry (**Figure 10b**) as well as for robust expression of a fusion CD-63 with increased molecular weight (**Figure 10c**).

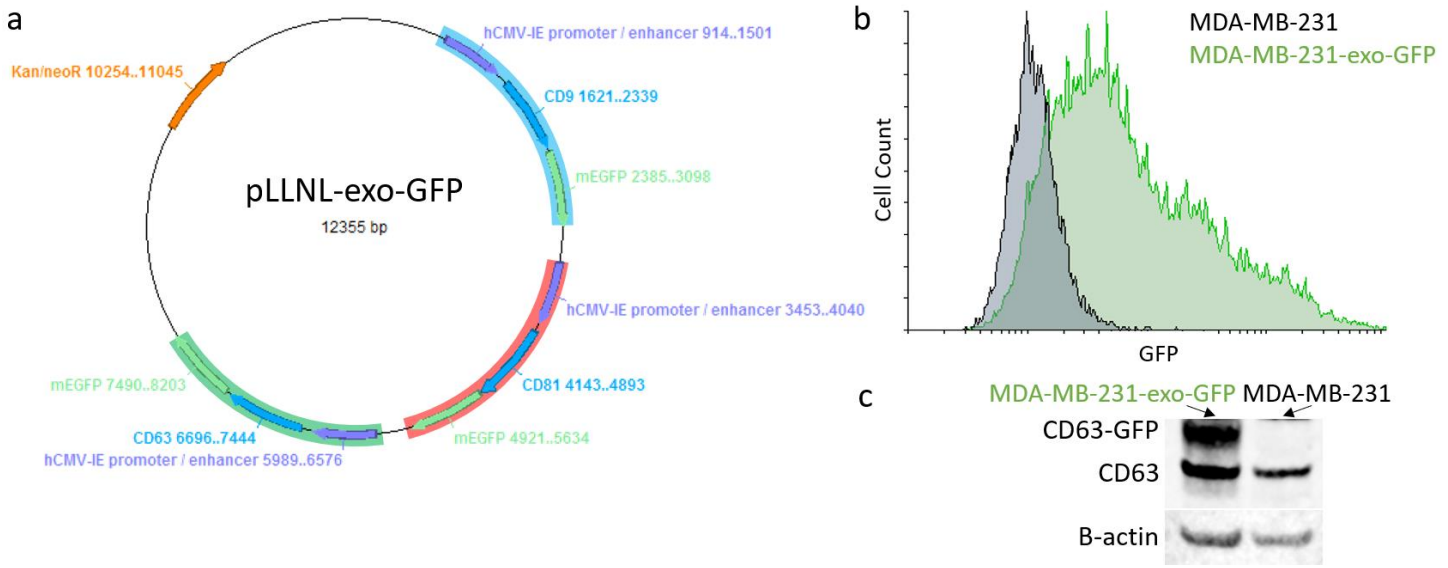

Figure 10: Genetic labeling of exosome populations. Transgenic construct with 3 tandem fusion proteins (a). Cell sorting of MDA-MB-231 transgenic stable line (b), protein expression of fusion protein, in transgenic MDA-MB-231 line MDA-MB-231-exo-GFP (c).

We next expanded the incorporation of our exosome labeling construct (pLLNL-exo-GFP) into remaining human cell lines. We successfully engineered a MDA-MB-231 cell line with a GFP fusion protein construct (**Figure 11**) as well as created new sublines of MCF-7-exo-GFP and MCF-10A-exo-GFP cancer cells. Through our initial success engineering a CD63-GFP fusion protein capable of fluorescently labeling ESVs, we devised a flow-cytometry based method to see if we could quantitatively track exosomes and their uptake in recipient cells. We were able to quantify exosome uptake in recipient cells at early timepoints (day 3 and day 14) and sequenced the RNA of those exosome-receiving cells using flow cytometry. This is an improvement over our originally proposed method as we are able to not only quantitatively track fluorescent exosome uptake, we were also able to study properties of recipient cells as this is a non-radiological based assay.

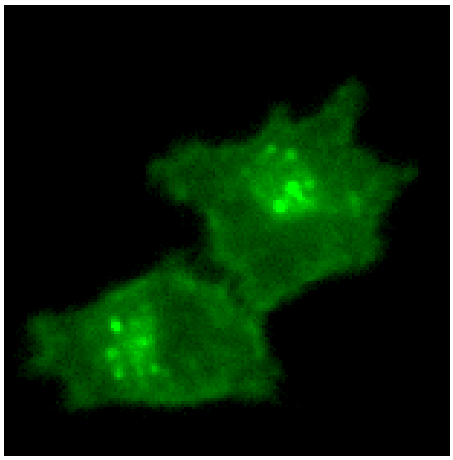

Figure 11. Representative images of transgenically labeled breast cancer cell lines, MDA-MB-231-exo-GFP.

Specific Aim 3: Use Accelerator Mass Spectrometry (AMS) technologies to quantify low levels of tumor derived RNA transferred via ESVs to osteoblasts and characterize their functions in promoting invasion.

Towards our goal of characterizing exosome function in promoting invasion, we (1) Tracked transfer of exosomes to recipient osteoblast cells using previously engineered MDA-MB-231-exo-GFP cell line; (2) Sequenced recipient osteoblast cells known to uptake MDA-MB-231-exo-GFP exosomes; (3) Isolated and characterized exosomes derived from all three breast cancer cell lines proposed: MCF-10A, MCF-7 and MDA-MB-231; (4) Sequenced exosome cargo and analyzed differences that relate to variation in cell line invasiveness; (5) Identified potential biomarkers packaged within highly invasive breast cancer exosomes that could be used to track disease progression

As referenced in Specific Aim #2, we have employed our genetically engineered MDA-MB-231-exo-GFP cell line to quantitatively track exosome uptake and sequence recipient cells.

In this study, we wanted to understand the transcriptional changes that take place following exposure to highly metastatic exosomes (MDA-MB-231-exo-GFP). First, we set up a co-culture transwell assay in which MDA-MB-231-exo-GFP cells were cultured on top of MC3T3 osteoblasts (recipient cells) (**Figure 12**). At 3 days and 14 days of culture, osteoblasts were sorted into GFP+ and GFP- populations and both osteoblast populations were sequenced.

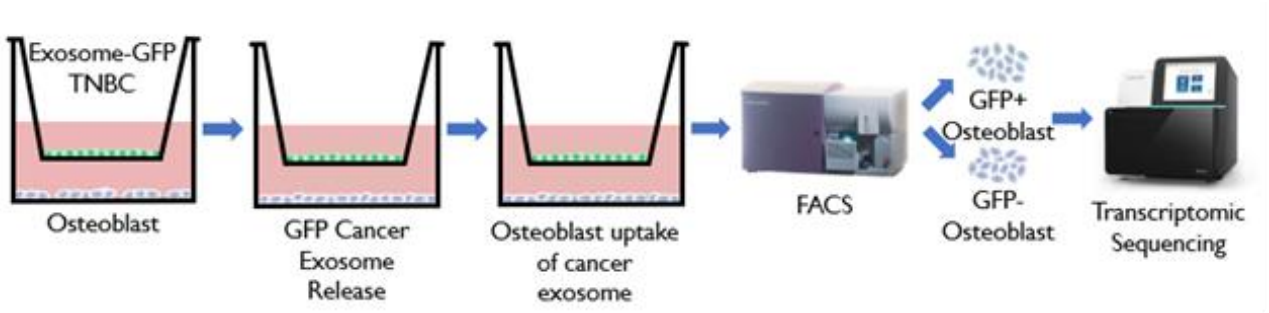

Figure 12. **Experimental design of co-culture experiment.** Transgenic human triple negative breast cancer (TNBC) MDA-MB-231 cells carrying pLLNL-exoGFP labeled exosomes containing CD9, CD63, or CD81 recombinant proteins were cultured on a transwell insert (pore size: 3 um) with murine osteoblast (MC3T3) cells for up to 14 days. Osteoblast cells that have uptaken GFP+ cancer exosomes were FACS sorted at day 3 and day 14 post initiation of co-culture. RNA was isolated from sorted population then RNA-seq was performed. Whole transcriptomic analysis was accomplished *via* pairwise analysis of positive vs negative populations at each time point.

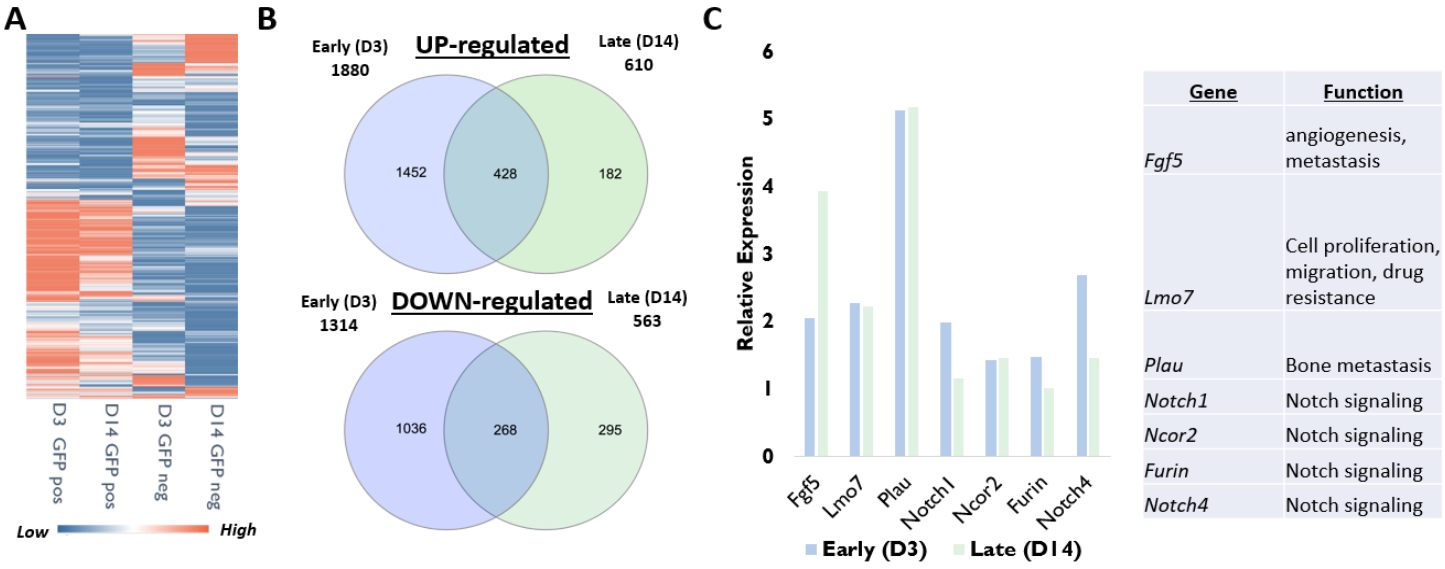

Gene	Function
Fgf5	angiogenesis, metastasis
Lmo7	Cell proliferation, migration, drug resistance
Plau	Bone metastasis
Notch1	Notch signaling
Ncor2	Notch signaling
Furin	Notch signaling
Notch4	Notch signaling

Figure 13. Transcriptional Changes in OBs fused to BC-derived exosomes. A) 2000 highly expressed genes are visualized to highlight transcriptional differences between GFPpos and GFPneg OBs purified from co-cultures. B) Venn Diagram showing numbers of UP- and DOWN-regulated transcripts and overlap between D3 and D14. C) Several genes known to affect cancer growth and metastasis were significantly upregulated in GFPpos OBs, and some of these genes belonged to the Notch family of signaling molecules [13-15].

To determine if information packaged within BC-derived EVs impacts gene expression in cells receiving the information *via* exosome-fusion, we co-cultured these transgenic cell lines with murine OBs (MC3T3) in transwell plates. The transwell pore size permitted exosome diffusion but not that of cancer cells. MC3T3 OBs were GFP^{neg} prior to co-culture and, only if they fused with a GFP^{pos} exosome shed by the BC cells, would become GFP^{pos}. OBs able to up-take GFP^{pos} cancer exosomes were sorted using FACS at days 3 (D3) and 14 (D14) post-initiation of the co-culture. While the update ranged between 3-5% of OBs, it was sufficient to sort and isolate RNA from the GFP^{pos} cells. RNA was isolated from sorted GFP^{pos} and GFP^{neg} OB populations and sequenced. Whole transcriptomic analysis was accomplished via pairwise analysis of GFP^{pos} and GFP^{neg} OB populations at each timepoint as described in **Figure 12**.

A heat map of the 2000 highest expressing genes from OBs co-cultured with MDA-MB-231 cells carrying pLLNL-exoGFP-labeled exosomes showed a clear distinction in gene expression between GFP^{pos} and GFP^{neg} OBs (**Figure 13A**). We found 1880 significantly upregulated genes at D3 post-co-culture and 610 significantly upregulated genes at D14 post-co-culture in GFP^{pos} OBs relative to GFP^{neg} OBs isolated from the same co-culture, suggesting that OBs receiving BC-derived exosomes are transcriptionally affected by the cargo packaged in these EVs. At D3 and D14, respectively, 1314 and 563 genes were significantly downregulated (**Figure 13B**). Pathway analyses of upregulated genes identified *interferon signaling* and *antigen processing-cross presentation* to be enriched at both time points. *Cytokine signaling in immune system, ECM synthesis, and cell-cell communication* pathways were significantly enriched at the early time point (D3), while genes corresponding to *rRNA processing* and *translation elongation and termination* pathways were significantly enriched at the later timepoint (D14) [16]. Interestingly, cancer-derived EV-induced changes in gene expression corresponded to genes associated with cancer progression. Consistent with published records, upregulation of genes known to influence cancer growth and metastasis were also significantly upregulated, and a few of these genes were members of the Notch signaling pathway (**Figure 13C**) [17] (Hum et al. 2020, *manuscript in preparation)*

To study the effect of breast cancer exosomes on invasion, we first characterized the physical properties of these extracellular vesicles. We characterized particle size of exosomes secreted by each of the three breast cancer cell lines using Nanoparticle Tracking Analysis. This technique utilizes positional information to mathematically calculate particle size and quantity (**Figure 14B**). This analysis revealed that exosomes derived from MCF-10A and MDA-MB-231 cells were similar in both size distribution as well as yield. MCF-10A and MDA-MB-231 cells produced particles approximately 350 nm in diameter while MCF-7 cells produced exosomes which were found to be smaller on average (~190 nm). Similarly, MCF-10A and MDA-MB-231 cells were also found to be similar when comparing amount of extracellular vesicle production. Both cell lines produced nearly three times less exosomes concentration when compared to MCF-7.

To determine what specific types of genetic cargo are packaged within extracellular vesicles we performed RNA sequencing of exosomal RNA derived from all three breast cancer cells lines. Exosomes were isolated from ~4.0×10^7 cells per replicate using a polymer-based precipitation method (ExoQuick-TC). System Bioscience performed sequencing library preparation using their Exo-NGS service then sequenced on an Illumina NextSeq550 using single end, 75-bp reads. Three replicates were sequenced per cell line. Based on sequencing analysis, we found that the differences in cell behavior and potential for invasiveness lie not so much in the distribution of type of cargo that is packaged, but the identity of the cargo itself. **Figure 14D** shows that approximately one third of the genes encoded in extracellular vesicles regardless of cell line of origin correspond to non-coding regions of the genome, whereas the remaining two-thirds relate to protein-coding genes. Further, the non-coding regions represent genes from a variety of small RNAs (miRNA, snoRNA, snRNA, miscRNA, rRNA) and others (pseudogenes, antisense, etc). Similarly, the distribution of small RNAs within exosomes derived from all three breast cancer cell lines was comparable. Taken together, this data suggests that phenotypic differences in how each of the breast cancer cell lines behave *in vitro* and *in vivo* can be attributed to the differences in gene expression of specific genes.

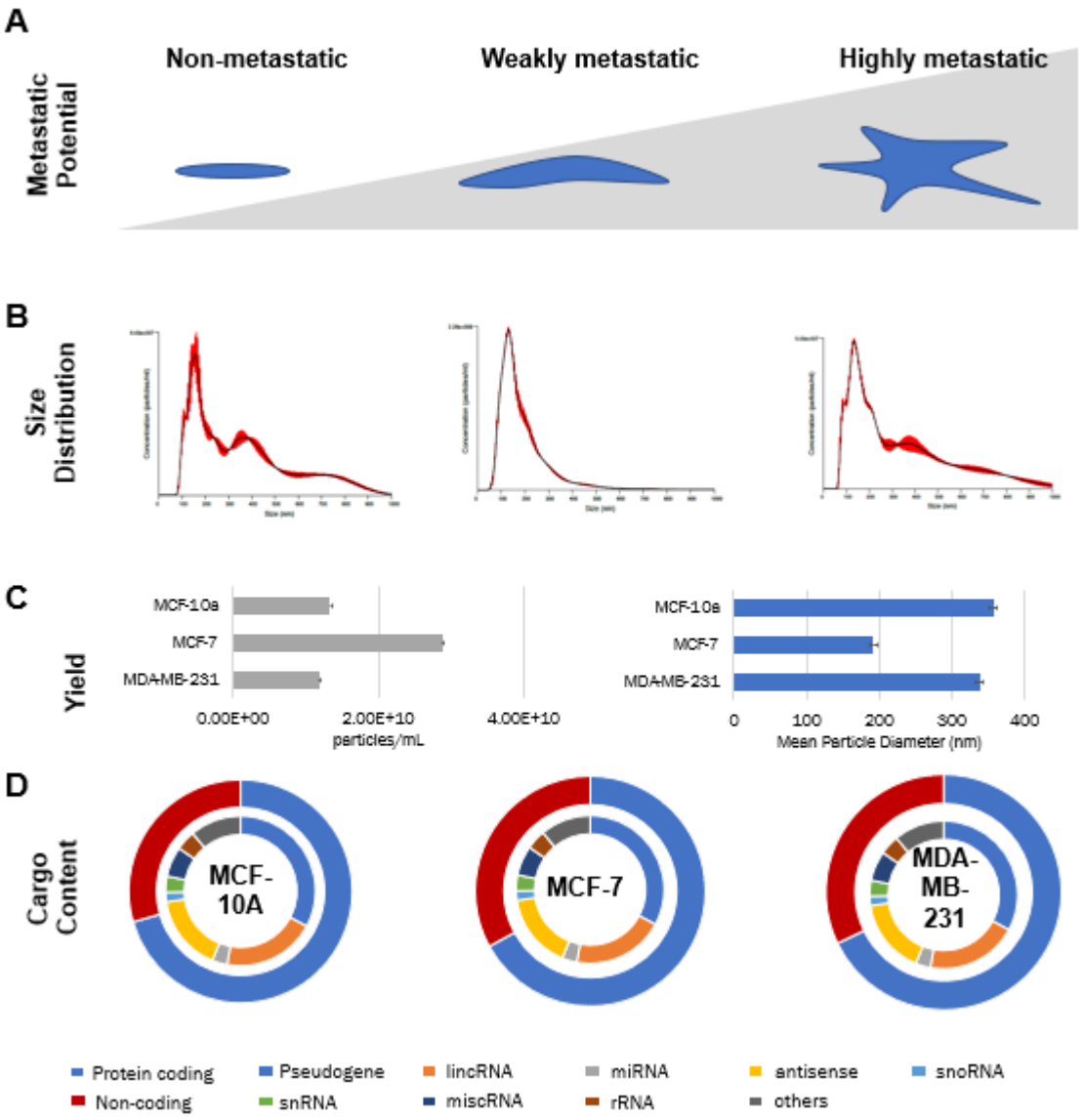

Figure 14. Exosome size and quantity characterization. Breast cancer exosomes were characterized using nanoparticle tracking analysis. Exosomes derived from MDA-MB-231 and MCF-10a cells were larger compared to those derived from MCF-7 cells. Additionally, MDA-MB-231 cells and MCF-10a cells produce statistically significantly less exosomes compared to MCF-7 cell line. N=3 replicates per cell type (A-C). A majority of RNA in exosomes align to coding regions of the genome (~70%) across all three cell lines. Non-coding RNA classification also shows little variability across cell lines examined regardless of metastatic potential (D).

Next, we wanted to distinguish between exosomes derived from metastatic cells (MCF-7) versus those from highly metastatic cells (MDA-MB-231) in both the number of non-coding genes differentially expressed as well as their identity (**Figure 15**). We found that there are 304 genes statistically significantly upregulated and 150 genes statistically significantly downregulated when comparing breast cancer exosomes (MCF-7 and MDA-MB-231) to normal, non-tumorigenic exosomes (MCF-10A). Interestingly, we found that that there are more differentially expressed genes between the MCF-7 compared to the MCF-10A exosomes than the MDA-MB-231 compared to the MCF-10A exosomes. This is likely due to the fact that both MDA-MB-231 cells and MCF-10A cells are derived from a similar gene cluster of triple negative breast cancer lineage.

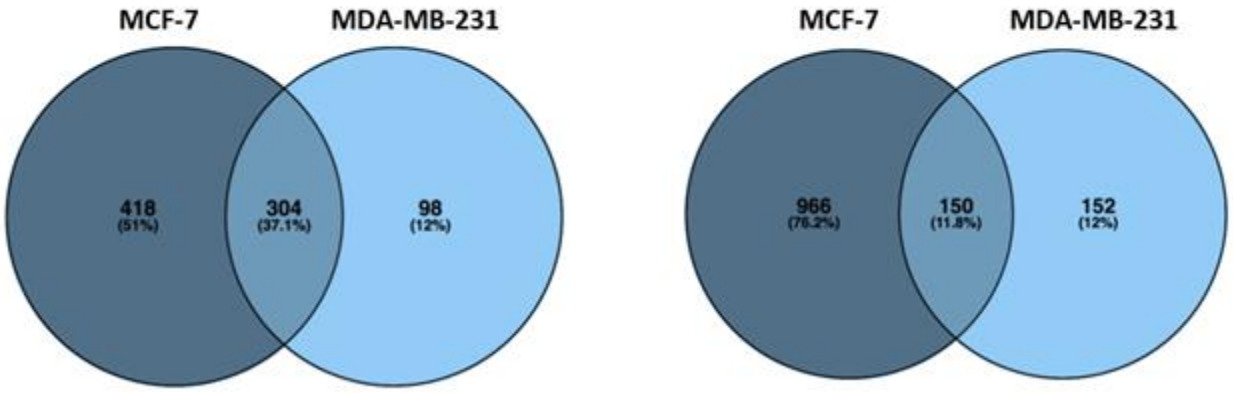

Figure 15. Up- and downregulated non-coding genes in breast cancer exosomes. Venn diagram representing the number of differentially expressed non-coding genes in exosomes from MDA-MB-231 cells and MCF-7 cells compared to MCF-10A.

Further investigating unique non-coding genes responsible for the metastatic versus the highly metastatic phenotype observed in the MCF-7 versus MDA-MB-231 cells respectively, we found the following microRNAs uniquely upregulated in MCF-7 exosomes (**Table 1**) and uniquely upregulated in MDA-MB-231 cells (Table 3). These microRNAs specific to metastatic and highly metastatic breast cancer can be further explored to evaluate specific function by which they confer a highly metastatic phenotype. Literature references shown in both **Table 1** and **Table 2** provide evidence of other research efforts aimed at identifying the role of each of these microRNAs. These references aim to validate our findings, showing that other studies have also concluded that these microRNAs are related to a pro-metastatic phenotype.

Table 1. Upregulated microRNAs unique to metastatic MCF-7 exosomes.

miRNA	Potential Role	Reference
miR-200a	Regulates EMT in lung cancer	Future Oncol. 2018 Sep 13, ahead of print
miR-3609	Regulates cell adhesion, MAPK signaling	Cell Physiol Biochem. 44(5):1923-38.
miR-375	Tumor suppressor, cancer initiation	Cancer Letters, 438:126-132.
miR-489	Regulates migration and invasion	Oncotarget, 8:36410-22.
miR-542	Tumor suppressor, regulates EMT transition via targeting survivin	Biomed Pharmacother, 99:817-24.
miR-7641-1	Potential biomarker for multiple cancers	Scientific Reports, 7:8365.
miR-9-3	Potential tumor suppressor, enhances apoptosis	Molecular Cancer, 12:173.

Next, we wanted to compare patterns of gene expression across exosomes derived from all three cells types to identify if there are any patterns of gene expression that follow a clinical breast cancer disease progression. Progress towards early diagnosis and successful cancer screening depends on useful biomarkers and molecular identifiers that can be detected minimally invasively. Towards this objective, we have identified 21 potential biomarkers where gene expression is statistically significantly upregulated from a non-tumorigenic model (MCF-10A to a metastatic model (MCF-7) and further upregulated in a highly invasive model (MDA-MB-231), indicative of late stage disease/metastasis (**Figure 16**).

Table 2. Upregulated microRNAs specific to highly metastatic MDA-MB-231 cells.

miRNA	Potential Role	Reference
miR-210	Upregulated in hypoxic environments, regulates EMT transition	Med Hypotheses. 84(3):209-12.
miR-646	Targets fibroblast growth factor 2 (FGF2)	Tumour Biol. 36(3):2127-34.
miR-668	Targets tumor suppressor gene (IKBa)	Breast Cancer. 24(5): 673-682.

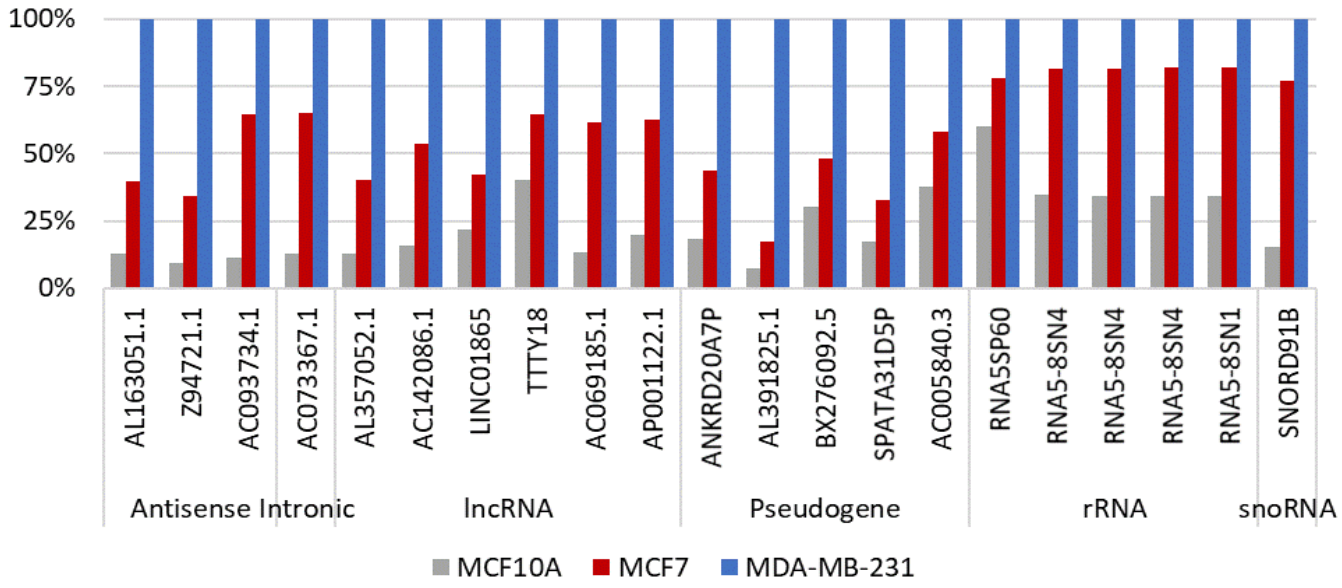

Figure 16. Potential candidate biomarkers based on patterns of gene expression in exosomes derived from cells of increasing invasiveness.

One limitation of using GFP for tracking exosomes *in vivo*, is that the GFP signal may be too weak to detect in cells that have fused with exosomes and that a more sensitive approach may be needed to transition the *in vitro* research to *in vivo* applications. To evaluate whether labeled exosomes could be robustly 'seen' in cells that have taken up exosome cargo, we conducted an experiment where BALB/c derived 3T3 fibroblasts were cultured for 48 hours in serum free media supplemented with 4T1 exosomes labeled by 2 different methods: 1) a green fluorescent, lipophilic carbocyanine dye that is widely used as a lipophilic tracer known as DiO dye and 2) ExoGlow™-Membrane EV Labeling Kit available from System Biosciences. The data obtained from these labeling techniques was then compared to the 3) transgene expression of GFP using pLLNL-exo-GFP transgene approach described above.

Characterization of exosome labeling dyes was performed to ensure low background and robust signal across several lipid and amine-based dyes. Lipophilic DiO (ThermoFisher Scientific) or proprietary exosome labeling dyes (NIR, ExoGlow-Vivo EV Labeling Kit, Systems Biosciences) were selected based on signal intensity and dye type for further exosome experiments. In order to examine optimal staining conditions, 4T1 (murine mammary carcinoma) derived exosomes isolated *via* ultracentrifugation were stained with either lipophilic DiO, or NIR, following manufacturer specifications. Unincorporated dye was eliminated using subsequent extracellular vesicle isolation for NIR stained cells or Exosome Spin Columns MW3000 (ThermoFisher

Scientific) for DiO stained cells. Subsequent analysis of supernatant and exosome negative staining controls was implemented to examine staining efficiency, level of detection, and prevalence of unincorporated dye into labeled exosome preparations have been optimized. The uptake of cancer derived exosomes in fibroblasts has been shown to play a role in fibroblast differentiation both in the local and premetastatic microenvironment [18-22] therefore we investigated the detection and uptake of 4T1 derived exosomes in BALB/c derived 3T3 fibroblast cells (ATCC). Following 48-hour incubation in serum free cell culture media supplemented with labeled BC derived exosomes, fibroblast cells were washed with PBS prior to ensure removal of non-bound exosomes. Cellular isolation was then performed using Accutase and cellular uptake was assayed with flow cytometry and fluorescence imaging of isolated cells suspensions.

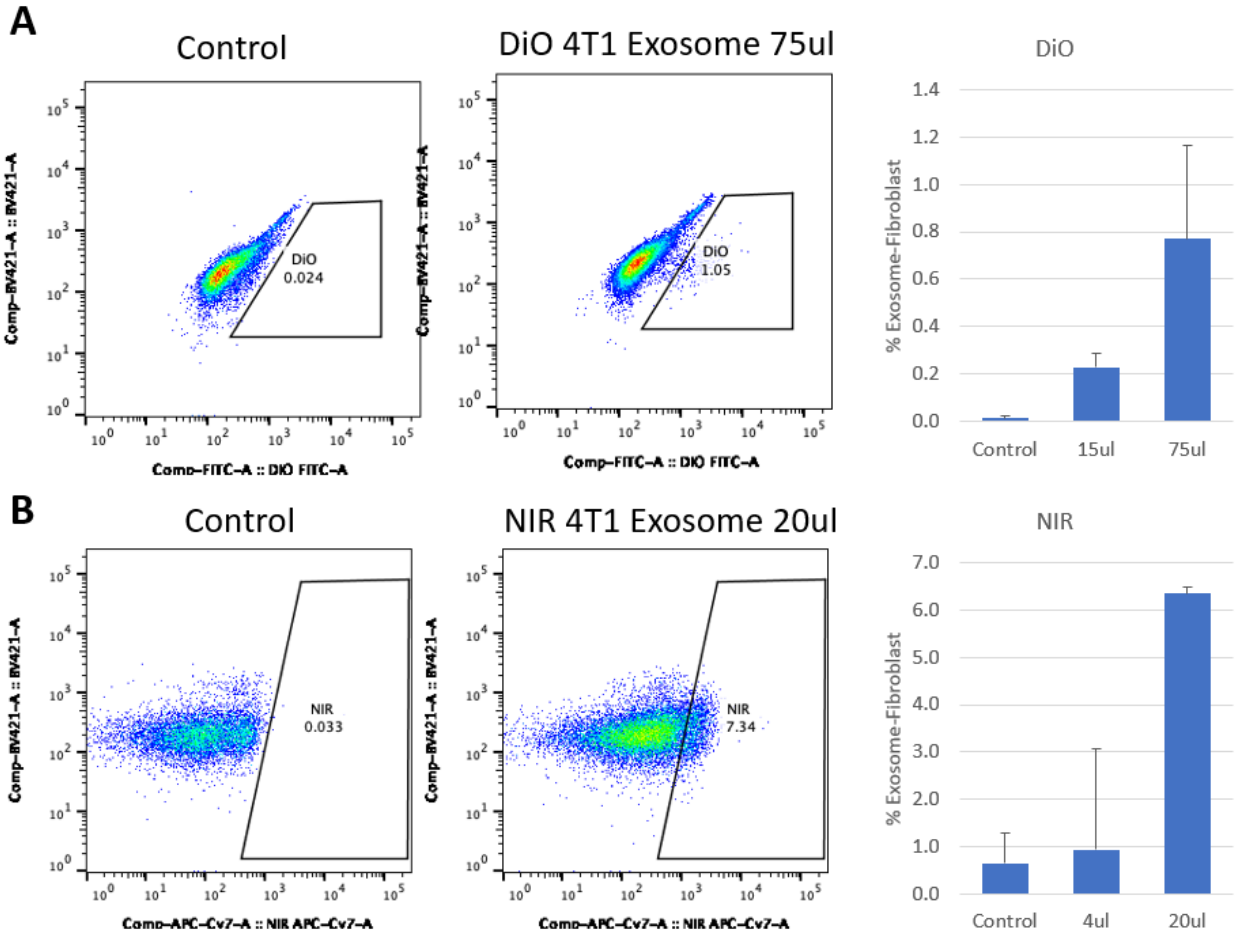

Figure 17. Comparing sensitivity of detecting exosome uptake, when 3T3 cells were exposed to exosomes labeled with (A) Lipophilic DiO or (B) NIR, ExoGlow.

Both dyes (DIO and NIR) were detectable in 3T3 fibroblasts (**Figure 17**), however lipid based DiO dye required >3-fold more exosomes to detect significant quantities of cells that fused to cancer exosomes. But even the largest amount administered (75ul) only resulted in ~1% labeling of 3T3 cells (**Figure 17A**). In contrast, NIR dye more robustly labeled 3T3 cells, and 20ul of exosomes administered to 3T3 fibroblasts, resulted in ~7% labeling of cells receiving exosomes (**Figure 17B**). This result was also superior to the co-culture experiment conducted with genetically encoded GFP, where in cancer-OB coculture experiments only 3-5% of co-cultured OBs became GFP+ after exposure to MDA-MB-231 cells carrying pLLNL-exoGFP labeled exosomes. These results suggest that administration of NIR labeled exosomes may allow us to identify cells within metastatic niches that fuse with cancer-derived exosomes.

One potential future direction of this work that was funded by this application is to pursue validation of our candidate biomarkers, as well as to conduct mechanistic studies that will aim to elucidate how metastasis is initiated. Such experiments will require that we can detect normal cells that have fused to cancer derived exosomes, *in vivo*. To determine whether *ex vivo* labeled exosomes with NIR dye can be detected *in vivo*, in

tissues that correspond to metastatic niches, NIR-labeled exosomes were administered *via* intracardiac injection into immune deficient, NOD-scid IL2Rgamma^{null} (NSG), mice. and 24 hours post injection, animals were euthanized, all tissues of interest were harvested, washed with PBS then imaged for biodistribution analysis using the NIR 800nm channel on an Odyssey FC system (Li-Cor Biosciences) . While 10 ul delivery resulted in no significant signal, 100 ul delivery showed robust signal in liver, lung and bone, tissues known to develop 4T1 metastatic lesions (**Figure 18**).

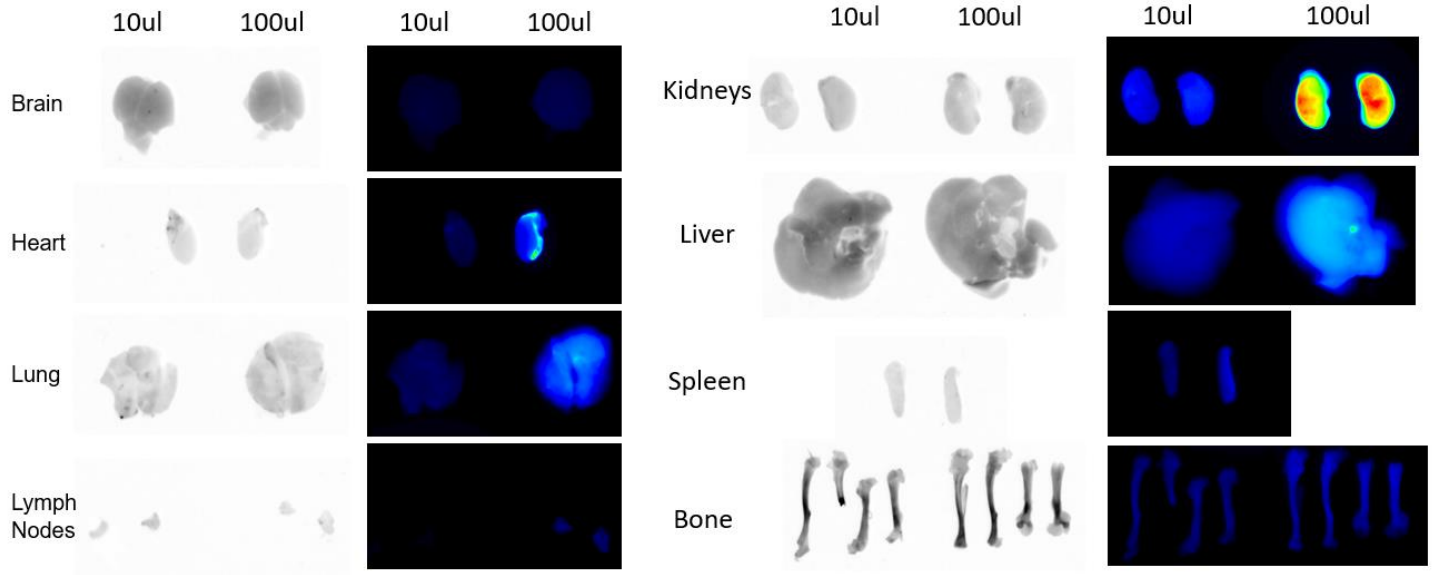

Figure 18. ***In vivo* update of exosomes labeled with NIR dye**. Two concentrations of NIR labeled 4T1-cancer cell derived exosomes were injected into immune deficient

Lastly, in future experiments we would like to evaluate the role of the immune system on metastasis, and conduct experiments in fully immune competent mice such as BALB/c mice. Such experiments can only be carried out with mouse cancer cell lines. To create new opportunities for studying metastasis in immune competent mice, we genetically modified 4T1 triple negative murine breast cancer cell line to express the exosome labeling trangene cassette described and developed under Aim1, and combined this transgene with a cell surface marker Thy1.1, that will also allow to distinguish cancer cells from normal cells, in allografts, using cell sorting. We generated two cell lines 4T1-Thy1, which had only the Thy1.1 marker, and 4T1-Thy1-ExoGFP which had both the cell surface Thy1.1 and the GFP-exosome labeling cassette. FACS sorting of monocultures of these 4T1 sublines, determined that ~84% of 4T1-Thy1-ExoGFP cells were brightly green (**Figure 19**). These cells will be used in future allograft experiments to identify stromal cells that fuse with 4T1-derived exosomes. Such stromal cells will be Thy1.1 negative and GFP positive, while the cancer cells will be Thy1.1 positive and GFP positive. Single cell sequencing will allow us to determine how cancer cells modify the stroma, to recruit healthy cells as cancer-supporting cells.

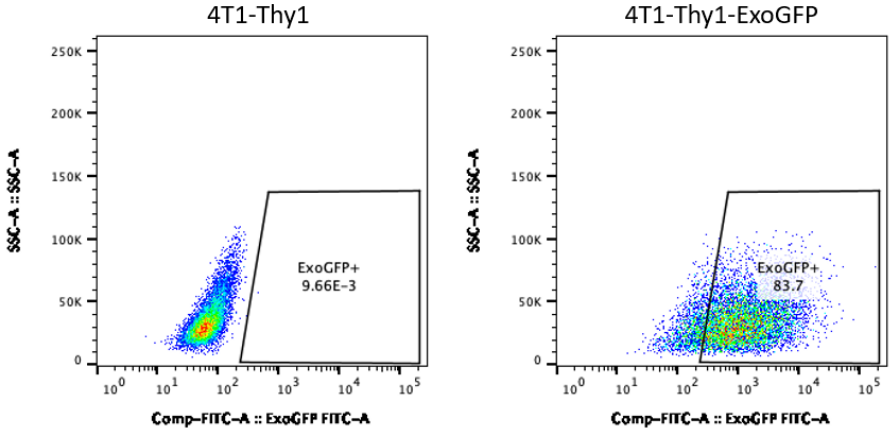

Figure 19. FACS detection and sorting of 4T1-Thy-ExoGFP cell line. ~84% of cells from a 4T1-Thy-ExoGFP established transgenic subline of 4T1 were GFP+ when compared to the 4T1-Thy1 parental cell line that had no detectable GFP cells.

- **What opportunities for training and professional development has the project provided?**

During the funding period, Kelly Martin was a graduate student from Georgetown University who conducted her Ph.D work at LLNL under Dr. Loots' mentorship. She allocated approximately 30% of her research efforts towards this project. She was involved with the isolation, characterization and fluorescent labeling of exosomes and microvesicles derived from various breast cancer cell lines. She also presented research and received insightful feedback from the research community in a variety of forums including the Annual Cancer Research Symposium held at UC Davis Comprehensive Cancer Center and the American Association for Cancer Research (AACR) annual meeting. Kelly is now a postdoc at LLNL.

Daniel Sosebee was a pre-college student who spent 3 months during the summer of FY17 [May 2017- July 2017] as an intern under Drs. Shusteff and Fong's mentorship. He thoroughly tested and characterized over 10 acoustophoretic separation chips that were subsequently used to isolate different extracellular vesicle populations. He determined the optimal frequency for separation and quantified the effect of different voltages on separation efficiency. He further assisted in identifying the conditions necessary to separate cells and cell debris from extracellular vesicles.

- **How were the results disseminated to communities of interest?**
    - Nicholas R. Hum, Kelly A. Martin, Aimy Sebastian, Gabriela G. Loots. *TRANSCRIPTOME ANALYSIS OF OSTEOBLASTS FUSED WITH CANCER-DERIVED EXOSOMES;* Poster Presentation at AACR Annual Meeting, Chicago, IL, 4/14-18, 2018
    - Nicholas R. Hum, Kelly A. Martin, Aimy Sebastian, and Gabriela G. Loots. *Comparison of breast cancer exosomes from cell lines of varying metastatic potential;* Poster Presentation UC Davis Cancer Center Symposium, Davis, CA 9/27-28, 2018
    - Nicholas R. Hum, Kelly A Martin, Gabriela G Loots. *Comparison of exosomes shed by breast cancer cell lines with varying metastatic potential*. Biotechnology MS Program. Oral presentation. Georgetown University Biotechnology Webinar Series: October 10, 2018.
    - Kelly A. Martin, Nicholas R. Hum, Aimy Sebastian, Gabriela G. Loots. Abstract 5157: *Comparison of exosomes shed by breast cancer cell lines with varying metastatic potential*. Poster Presentation. Conference: Proceedings: AACR Annual Meeting; March 29-April 3, 2019; Atlanta, GA.
    - Nicholas R. Hum, Kelly A. Martin, Aimy Sebastian, Gabriela G. Loots. Metastatic breast cancer derived extracellular vesicles contribute to cancer progression and induce cancer associated fibroblast differentiation. Molecular Cancer Research. 2020. Manuscript *in preparation*
- **What do you plan to do during the next reporting period to accomplish the goals?**
    - Grant has completed, expansion award has been submitted to continue this work and pursue *in vivo* validation

- **IMPACT:** *Describe distinctive contributions, major accomplishments, innovations, successes, or any change in practice or behavior that has come about as a result of the project relative to:*
- **What was the impact on the development of the principal discipline(s) of the project?**
    - *When attending AACR we got requests for protocols, vectors and positive feedback on our work.*
- **What was the impact on other disciplines?**
    - *The vectors we made can be used to study exosome trafficking in many other contexts, we have had requests for collaboration from scientists (Drs. Damian Genetos and Claire Yellowley at UC*

Davis) who are interested in fracture repair, to study how muscle and stem cells may shed exosomes to contribute to bone healing.

- **What was the impact on technology transfer?**
    - *We have made vectors available to other investigators through Material Transfer Agreements.*
- **What was the impact on society beyond science and technology?**
    - *Nothing to Report*

- **CHANGES/PROBLEMS:** *The Project Director/Principal Investigator (PD/PI) is reminded that the recipient organization is required to obtain prior written approval from the awarding agency Grants Officer whenever there are significant changes in the project or its direction. If not previously reported in writing, provide the following additional information or state, "Nothing to Report," if applicable:*
    - **Changes in approach and reasons for change**

In the original proposal we aimed to isolate large oncosome populations (> 5 μm) from smaller microvesicle and exosome populations using immunological beads combined with acoustic separation. Our proposed experimental plan using acoustic separation to isolate large oncosomes and immunologically-labeled vesicle subsets in a single device was expected to streamline vesicle purification (Tasks 1b and 1c). Separation of bio-particles using acoustophoresis was less efficient for smaller sized particles. Focusing and separation degrades steeply as the particle size nears 1 μm due to competing acoustic streaming effects which increase mixing. Given the fundamental limitations of acoustophoresis to isolate different ESV populations <1 μm, it was necessary to use immunological beads to increase the size and contrast factor of bound ESVs. However, we determined that using acoustophoretic separation with immunological beads was not superior to existing immunological ESV purification methods using magnetic beads. Existing methods using functionalized magnetic beads was superior in throughput as well as limiting the dilution of exosome samples. In our original proposal we expected acoustophoresis to be an ideal label free method for isolating populations of large oncosomes, but since we were unable to “find” oncosomes, we determined that pursuing acoustophoresis for isolation of small ESV populations was futile and unlikely to improve upon existing methods. Therefore, we chose to shift our focus towards identifying label-free methods of concentrating and purifying exosomes. In our last report, we detailed the separation parameters for purifying ESVs vs host/cell debris. However, since we determined our method to isolate ESVs was not superior to established immunologic magnetic bead assays, we instead pursued evaluation of several other ESV isolation and purification techniques. We investigated three methods of vesicle concentration and purification: 1) Ultracentrifugation, the gold standard for exosome isolation[3], 2) ExoQuick, an ethylene glycol precipitation-based method, and 3) InnovaPrep’s Concentrating Pipette, an emerging filtration-based technique, which isolates particles on size selective filters and then recovers them using a high-pressure aerosol elution foam designed to gently and completely remove particles from the membrane. We anticipate comparing concentration, recovery and morphology of ESVs isolated using each of these techniques. However, none of these methods proved superior to ultracentrifugation, therefore we applied ultracentrifugation to all experiments in Aims 2 and 3.

- **Actual or anticipated problems or delays and actions or plans to resolve them**

Since we were seeking to develop a new method of ESV purification and concentration, we anticipate that the development will take longer than building off our existing acoustophoretic separation device. We hoped to develop a platform which would be compatible with commercial filter membranes, to enable different types of membranes with different selectivity (size, charge, etc.) to isolate different ESV populations. However, since this new development effort did not prove to be superior to ultracentrifugation, the scope of the project was slightly changed to focus on whole population ESV purification and concentration, rather than trying to separate different sub populations.

- **Changes that had a significant impact on expenditures**
    - *No*

- **Significant changes in use or care of human subjects, vertebrate animals, biohazards, and/or select agents**
    - *After the funding period ended, an in vivo animal experiment was carried out with exosomes stored in our freezer. These exosomes were harvested and labeled in vitro, during the FY19 funding period of this grant. The exosomes were injected into mice under an approved LLNL IACUC protocol, using internal LLNL funds, and this data is presented in Figure 14. The animal experiment was NOT part of this grant and was funded by an internal LLNL grant to Dr. Elizabeth Wheeler. The data obtained from this in vivo experiment bears such significance that we chose to include it in this final report to illustrate future directions and impact of the work conducted under this grant.*
- **Significant changes in use or care of human subjects**
    - *Not applicable*
- **Significant changes in use or care of vertebrate animals.**
    - *Not applicable*
- **Significant changes in use of biohazards and/or select agents**
    - *Not applicable*
-

- **PRODUCTS:** *List any products resulting from the project during the reporting period. If there is nothing to report under a particular item, state "Nothing to Report."*
    - *Nothing to Report*
-

- **PARTICIPANTS & OTHER COLLABORATING ORGANIZATIONS**
    - **What individuals have worked on the project?**
        - *Provide the following information for: (1) PDs/PIs; and (2) each person who has worked at least one person month per year on the project during the reporting period, regardless of the source of compensation (a person month equals approximately 160 hours of effort). If information is unchanged from a previous submission, provide the name only and indicate "no change."*

Name:	*Gabriela G Loots*
Project Role:	*PI*
Researcher Identifier (e.g. ORCID ID):	0000-0001-9546-5561
Nearest person month worked:	*1*
Contribution to Project:	*Dr. Loots was in charge of overseeing the project and collaboration with engineering group, met with team regularly [weekly] to discuss experimental design, data analysis, troubleshooting and future directions*
Funding Support:	*n/a*

Name:	*Maxim Shusteff*
Project Role:	*Co-PI*
Researcher Identifier (e.g. ORCID ID):	
Nearest person month worked:	*1*
Contribution to Project:	*Dr. Shusteff was in charge of overseeing the engineering component of this project, met with team regularly [weekly] to discuss experimental design, data analysis, troubleshooting and future directions*
Funding Support:	*n/a*

Name:	*Erika Fong*
Project Role:	*Postdoctoral Fellow*
Researcher Identifier (e.g. ORCID ID):	
Nearest person month worked:	*3*
Contribution to Project:	*Dr. Fong conducted all engineering, microfluidic experiments, met with the biologists regularly, optimized experimental design, collected data, analyzed data, troubleshooting*
Funding Support:	*n/a*

Name:	*Nicholas Hum*
Project Role:	*Biomedical scientist*
Researcher Identifier (e.g. ORCID ID):	0000-0003-1605-3193
Nearest person month worked:	*1.5*
Contribution to Project:	*Mr. Hum in a biologist, he conducted cloning, culturing the cells, transfecting the cells, carrying our FACs analysis, isolating ESV via centrifugation*
Funding Support:	*n/a*

Name:	*Kelly Martin*
Project Role:	*Graduate Student*
Nearest person month worked:	3
Contribution to Project:	*Ms. Martin is a graduate student and has performed ESV isolation via ultracentrifugation, ESV characterization and cell culture.*
Funding Support:	*Livermore Graduate Scholar Fellowship*

Name:	*Deepa Murugesh Sosebee*
Project Role:	*Lab Technician*
Nearest person month worked:	*6*
Contribution to Project:	*Assisted with cell culture, FACS sorting, RNA isolation*
Funding Support:	*n/a*

Name:	*Aimy Sebastian*
Researcher Identifier (e.g. ORCID ID):	0000-0002-7822-7040
Project Role:	*Postdoctoral Fellow*
Nearest person month worked:	*1*
Contribution to Project:	*Assisted with RNAseq analysis*
Funding Support:	*n/a*

- **Has there been a change in the active other support of the PD/PI(s) or senior/key personnel since the last reporting period?**
    - *Nothing to Report*
- **What other organizations were involved as partners?**
    - *Nothing to Report*

References Cited

1. Lobb, R. J.; Becker, M.; Wen, S. W.; Wong, C. S.; Wiegmans, A. P.; Leimgruber, A.; Moller, A., Optimized exosome isolation protocol for cell culture supernatant and human plasma. *J Extracell Vesicles* **2015,** 4, 27031.
2. Li, P.; Kaslan, M.; Lee, S. H.; Yao, J.; Gao, Z., Progress in Exosome Isolation Techniques. *Theranostics* **2017,** 7, (3), 789-804.
3. Cheung, L. S.; Sahloul, S.; Orozaliev, A.; Song, Y. A., Rapid Detection and Trapping of Extracellular Vesicles by Electrokinetic Concentration for Liquid Biopsy on Chip. *Micromachines (Basel)* **2018,** 9, (6).
4. Musante, L.; Tataruch, D.; Gu, D.; Benito-Martin, A.; Calzaferri, G.; Aherne, S.; Holthofer, H., A simplified method to recover urinary vesicles for clinical applications, and sample banking. *Sci Rep* **2014,** 4, 7532.
5. Liang, L. G.; Kong, M. Q.; Zhou, S.; Sheng, Y. F.; Wang, P.; Yu, T.; Inci, F.; Kuo, W. P.; Li, L. J.; Demirci, U.; Wang, S., An integrated double-filtration microfluidic device for isolation, enrichment and quantification of urinary extracellular vesicles for detection of bladder cancer. *Sci Rep* **2017,** 7, 46224.

6. Woo, H. K.; Sunkara, V.; Park, J.; Kim, T. H.; Han, J. R.; Kim, C. J.; Choi, H. I.; Kim, Y. K.; Cho, Y. K., Exodisc for Rapid, Size-Selective, and Efficient Isolation and Analysis of Nanoscale Extracellular Vesicles from Biological Samples. *ACS Nano* **2017,** 11, (2), 1360-1370.
7. Zhang, J. Y.; Mahalanabis, M.; Liu, L.; Chang, J.; Pollock, N. R.; Klapperich, C. M., A Disposable Microfluidic Virus Concentration Device Based on Evaporation and Interfacial Tension. *Diagnostics (Basel)* **2013,** 3, (1), 155-69.
8. Zhang, H.; Tiggelaar, R. M.; Schlautmann, S.; Bart, J.; Gardeniers, H., In-line sample concentration by evaporation through porous hollow fibers and micromachined membranes embedded in microfluidic devices. *Electrophoresis* **2016,** 37, (3), 463-71.
9. Choi, J. W.; Hosseini Hashemi, S. M.; Erickson, D.; Psaltis, D., A micropillar array for sample concentration via in-plane evaporation. *Biomicrofluidics* **2014,** 8, (4), 044108.
10. Ho, N. T.; Fan, A.; Klapperich, C. M.; Cabodi, M., Sample concentration and purification for point-of-care diagnostics. *Conf Proc IEEE Eng Med Biol Soc* **2012,** 2012, 2396-9.
11. Fong, E. J.; Huang, C.; Hamilton, J.; Benett, W. J.; Bora, M.; Burklund, A.; Metz, T. R.; Shusteff, M., A Microfluidic Platform for Precision Small-volume Sample Processing and Its Use to Size Separate Biological Particles with an Acoustic Microdevice. *J Vis Exp* **2015**, (105).
12. Andreu, Z.; Yanez-Mo, M., Tetraspanins in extracellular vesicle formation and function. *Front Immunol* **2014,** 5, 442.
13. Meurette, O.; Mehlen, P., Notch Signaling in the Tumor Microenvironment. *Cancer Cell* **2018,** 34, (4), 536-548.
14. Cai, H.; Lu, W.; Zhang, Y.; Liu, H.; Wang, Z.; Shen, Y., Specific inhibition of Notch1 signaling suppresses properties of lung cancer stem cells. *J Cancer Res Ther* **2019,** 15, (7), 1547-1552.
15. Li, L.; Tang, P.; Li, S.; Qin, X.; Yang, H.; Wu, C.; Liu, Y., Notch signaling pathway networks in cancer metastasis: a new target for cancer therapy. *Med Oncol* **2017,** 34, (10), 180.
16. de Klerk, E.; t Hoen, P. A., Alternative mRNA transcription, processing, and translation: insights from RNA sequencing. *Trends Genet* **2015,** 31, (3), 128-39.
17. Zhang, J.; Kuang, Y.; Wang, Y.; Xu, Q.; Ren, Q., Notch-4 silencing inhibits prostate cancer growth and EMT via the NF-kappaB pathway. *Apoptosis* **2017,** 22, (6), 877-884.
18. Ringuette Goulet, C.; Bernard, G.; Tremblay, S.; Chabaud, S.; Bolduc, S.; Pouliot, F., Exosomes Induce Fibroblast Differentiation into Cancer-Associated Fibroblasts through TGFbeta Signaling. *Mol Cancer Res* **2018,** 16, (7), 1196-1204.
19. Antonyak, M. A.; Li, B.; Boroughs, L. K.; Johnson, J. L.; Druso, J. E.; Bryant, K. L.; Holowka, D. A.; Cerione, R. A., Cancer cell-derived microvesicles induce transformation by transferring tissue transglutaminase and fibronectin to recipient cells. *Proc Natl Acad Sci U S A* **2011,** 108, (12), 4852-7.
20. Webber, J.; Steadman, R.; Mason, M. D.; Tabi, Z.; Clayton, A., Cancer exosomes trigger fibroblast to myofibroblast differentiation. *Cancer Res* **2010,** 70, (23), 9621-30.
21. Fang, T.; Lv, H.; Lv, G.; Li, T.; Wang, C.; Han, Q.; Yu, L.; Su, B.; Guo, L.; Huang, S.; Cao, D.; Tang, L.; Tang, S.; Wu, M.; Yang, W.; Wang, H., Tumor-derived exosomal miR-1247-3p induces cancer-associated fibroblast activation to foster lung metastasis of liver cancer. *Nat Commun* **2018,** 9, (1), 191.
22. Naito, Y.; Yamamoto, Y.; Sakamoto, N.; Shimomura, I.; Kogure, A.; Kumazaki, M.; Yokoi, A.; Yashiro, M.; Kiyono, T.; Yanagihara, K.; Takahashi, R. U.; Hirakawa, K.; Yasui, W.; Ochiya, T., Cancer extracellular vesicles contribute to stromal heterogeneity by inducing chemokines in cancer-associated fibroblasts. *Oncogene* **2019,** 38, (28), 5566-5579.